

# VividFace: High-Quality and Efficient One-Step Diffusion For Video Face Enhancement

Shulian Zhang<sup>1\*</sup> Yong Guo<sup>2\*</sup> Long Peng<sup>3\*</sup>  
 Ziyang Wang<sup>1</sup> Ye Chen<sup>1</sup> Wenbo Li<sup>4</sup>  
 Xiao Zhang<sup>5</sup> Yulun Zhang<sup>6</sup> Jian Chen<sup>2†</sup>

<sup>1</sup>South China University of Technology

<sup>2</sup>Max Planck Institute for Informatics

<sup>3</sup>University of Science and Technology of China

<sup>4</sup>The Chinese University of Hong Kong

<sup>5</sup>Nanjing University of Science and Technology

<sup>6</sup>Shanghai Jiao Tong University

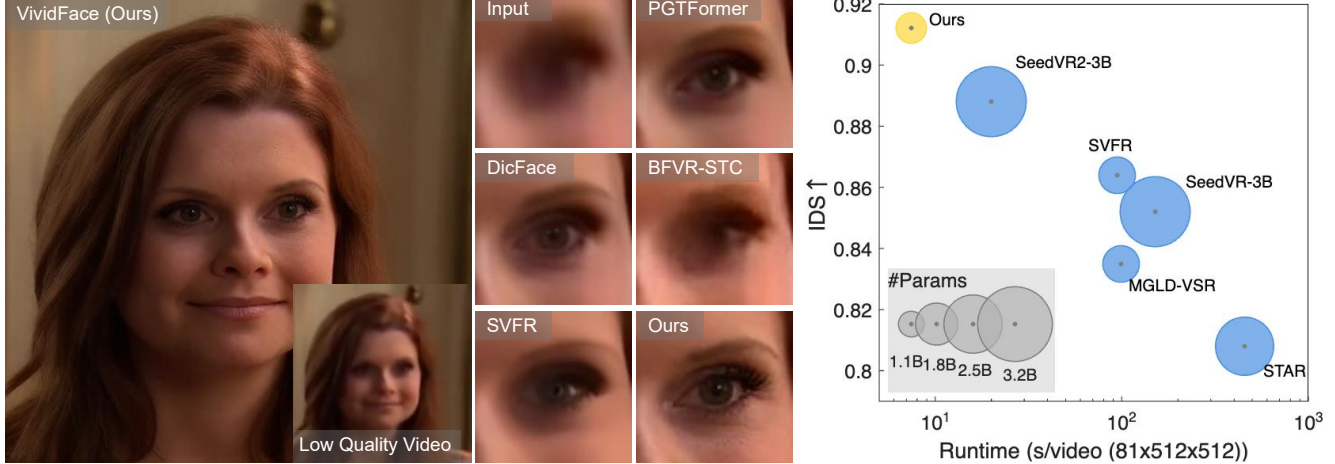


Figure 1. The left side shows a visual comparison between VividFace and existing video face restoration methods, illustrating that VividFace produces highly realistic and visually pleasing human eyes. The right side compares model inference time, parameter count, and IDS performance across different methods. VividFace achieves best performance, fastest speed, and comparable model parameter.

## Abstract

*Video Face Enhancement (VFE) aims to restore high-quality facial regions from degraded video sequences, enabling a wide range of practical applications. Despite substantial progress in the field, current methods that primarily rely on video super-resolution and generative frameworks continue to face three fundamental challenges: (1) computational inefficiency caused by iterative multi-step denoising in diffusion models; (2) faithfully modeling intricate facial textures while preserving temporal consistency; and (3) limited model generalization due to the lack of high-quality face video training data. To address these chal-*

*lenges, we propose **VividFace**, a novel and efficient one-step diffusion framework for VFE. Built upon the pretrained WANX video generation model, VividFace reformulates the traditional multi-step diffusion process as a single-step flow matching paradigm that directly maps degraded inputs to high-quality outputs with significantly reduced inference time. To enhance facial detail recovery, we introduce a Joint Latent-Pixel Face-Focused Training strategy that constructs spatiotemporally aligned facial masks to guide optimization toward critical facial regions in both latent and pixel spaces. Furthermore, we develop an MLLM-driven automated filtering pipeline that produces MLLM-Face90, a meticulously curated high-quality face video dataset, en-*

suring models learn from photorealistic facial textures. Extensive experiments demonstrate that **VividFace** achieves superior performance in perceptual quality, identity preservation, and temporal consistency across both synthetic and real-world benchmarks. We will publicly release our code, models, and dataset to support future research.

## 1. Introduction

Video face enhancement (VFE) aims to remove degradations and restore fine details in facial videos. It has become a fundamental technology for diverse applications such as surveillance systems, film restoration, video communication platforms, and digital content creation [23, 37, 52]. The core challenge in VFE lies in accurately modeling facial textures and reconstructing realistic details while ensuring efficient processing of video sequences. Recent advances in deep learning have driven the development of numerous VFE methods [4, 11, 27, 37, 40, 46, 47, 55], which have shown encouraging performance improvements.

Despite this progress, current VFE methods still face three fundamental limitations. First, although diffusion-based approaches have demonstrated strong generative capabilities for high-fidelity reconstruction, they suffer from significant inference efficiency bottlenecks. Their iterative multi-step sampling processes [27, 40, 47, 55] making them impractical for real-time or large-scale deployment scenarios where processing speed is critical. Second, existing methods often struggle to recover sufficient facial details [4, 37, 46], particularly failing to reconstruct fine-grained textures in critical areas like eyes and lips. This limitation results in visually blurred or unnatural facial appearances, as illustrated in Figure 1. Third, widely used public datasets such as VoxCeleb1 [19] and VFHQ [43] exhibit inherent quality limitations, containing videos with inconsistent degradations including motion blur, poor illumination, and facial occlusions. These data quality issues fundamentally impede the effective learning of authentic facial texture structures, limiting model generalization capabilities.

To address these limitations, we introduce **VividFace**, an efficient one-step diffusion framework for video face enhancement. Building upon the advanced text-to-video generation model WANX [29], we leverage its robust spatiotemporal priors while reformulating the traditional multi-step diffusion process into a single-step paradigm using flow matching [9]. This reformulation enables direct and effective mapping from degraded inputs to high-quality outputs, achieving a substantial 12 $\times$  speedup over SVFR [40] while maintaining superior visual fidelity and temporal consistency. Recognizing that facial regions contain the most perceptually critical features, we propose a Joint Latent-Pixel Face-Focused Training strategy that constructs spatiotemporally aligned facial masks to explicitly guide model

optimization toward key facial areas in both latent and pixel spaces. Furthermore, to address the data quality challenges prevalent in existing face-centric datasets, we develop a high-quality video filtering pipeline driven by a Multimodal Large Language Model (MLLM). This pipeline automatically assesses multiple quality dimensions through carefully crafted prompts, producing our curated MLLM-Face90 dataset that ensures photorealistic facial texture learning. Extensive experiments on both synthetic and real-world datasets demonstrate the superior performance of our approach compared to existing methods.

We summarize our contributions as follows:

- We introduce the first one-step diffusion framework tailored for video face enhancement, achieving a remarkable 12 $\times$  speedup over SVFR while consistently outperforming existing methods across diverse evaluation metrics on both synthetic and real-world datasets.
- We propose a novel Joint Latent-Pixel Face-Focused Training strategy, which provides explicit facial guidance in both latent and pixel spaces, enabling more targeted optimization of facial regions through a progressive two-stage training process.
- We develop an automated MLLM-driven high-quality video filtering pipeline and present MLLM-Face90, a meticulously curated dataset containing 1,957 high-quality face video clips, empowering the model to learn more authentic facial textures and details.

## 2. Related Work

**Video Face Enhancement.** Face video enhancement aims to recover high-quality facial video from degraded video, and finds application in surveillance, entertainment, and video communication scenarios. Directly applying general image and video enhancement methods [2, 3, 15, 16, 20, 21, 32, 34, 36, 44, 48] often leads to suboptimal results. Recent research has focused on dedicated face video enhancement approaches to address unique challenges such as inter-frame flickering, identity drift, and texture inconsistencies. PGT-Former [46] is the first method tailored for video face enhancement, enabling end-to-end enhancement without pre-alignment. KEEP [11] improves temporal consistency by recursively leveraging previously restored frames to guide current frame enhancement. SVFR [40] utilizes generation and motion priors from Stable Video Diffusion for more robust enhancement. DicFace [4] introduces the Dirichlet distribution for continuous codebook combination, offering greater flexibility in representation. Furthermore, current methods are still limited by the low quality of available data. Although existing datasets such as VoxCeleb1 [19], CelebV-HQ [54], VFHQ [43], and FOS [5] provide a large amount of facial video data, these datasets often contain degradations such as motion blur, poor lighting, and occlusions, resulting in suboptimal training data quality. These

low-quality data samples pose significant challenges for face enhancement methods, making it difficult to efficiently generate realistic facial textures.

**One-step Diffusion.** Diffusion models [12, 22, 24, 25] have achieved impressive visual results in various tasks, thanks to their ability to generate high-fidelity and realistic frames. However, their multi-step inference process leads to high computational cost and slow generation, especially for video data where efficiency is crucial. Recently, one-step diffusion methods have been proposed to accelerate generation, and have shown promising results in both image [8, 14, 35, 42] and video super-resolution [6, 17, 26, 31]. Despite these advances, the application of one-step diffusion remains largely unexplored for blind face video enhancement, leaving a gap in this important area.

### 3. Efficient Video Face Enhancement

In the following, we focus on addressing the key challenges in video face enhancement: computational inefficiency of multi-step diffusion models, insufficient facial detail reconstruction, and limited training data quality. First, we reformulate multi-step diffusion into an efficient one-step flow to accelerate inference (Section 3.1). Next, we introduce a Joint Latent–Pixel Face-Focused Training strategy that explicitly concentrates learning on key facial regions (Section 3.2). Finally, we design an MLLM-driven high-quality video filtering pipeline to automatically curate face-centric training data with superior quality (Section 3.3).

#### 3.1. One Step Flow Matching

Multi-step diffusion models suffer from significant computational overhead due to iterative sampling, hindering their real-time deployment. To address this bottleneck, we reformulate the diffusion process into a one-step flow matching framework built upon WANX [29], a powerful pre-trained text-to-video generation model. WANX employs an encoder-DiT-decoder architecture and is pretrained on large-scale real-world video datasets via multi-step flow matching, thereby providing robust spatiotemporal generative priors. Leveraging these priors, our method effectively adapts WANX to handle diverse degradation patterns in face video enhancement. Critically, since degraded face videos already retain sufficient structural information, we reformulate the multi-step process into a direct single-step transformation that maps low-quality inputs to high-quality outputs. This design achieves a remarkable 12 $\times$  speedup over SVFR while maintaining superior visual quality (see Table 3).

The overall architecture is illustrated in Fig. 2. Following Rectified Flows [9], given a low-quality face video  $x_l$ , we first encode it into a latent representation  $z_l$  using the VAE encoder  $\mathcal{E}$ . We designate  $z_l$  as the flow starting point and define a linear flow trajectory between degraded input  $z_l$

and high-quality target  $z_h$ , as follows:

$$z_t = (1 - t)z_l + tz_h, \quad t \in [0, 1], \quad (1)$$

where  $t$  represents the time step. The target velocity field is then given by:

$$v_t = \frac{dz_t}{dt} = z_h - z_l. \quad (2)$$

The DiT model  $v_\theta$  is trained to predict this velocity field  $v_t$  through a single denoising step, generating high-quality latent  $\hat{z}_h$ , as follows:

$$\hat{z}_h = z_l + v_\theta(z_l, t^*, c_{txt}), \quad (3)$$

where  $c_{txt}$  represents the text embedding and  $t^*$  is the fixed timestep. To facilitate efficient training of the DiT, we precompute the latent representations of both low- and high-quality videos using the VAE encoder and adopt empty text prompts to eliminate caption-related computational overhead. Empirically, we set  $t^* = 400$  in the original discrete timestep scale (corresponding to  $t \approx 0.4$  in the continuous scale), which balances structural preservation and detail enhancement based on the observation that the low-resolution input already contains sufficient structural information. Finally, the enhanced latent representation  $\hat{z}_h$  is decoded by the VAE decoder  $\mathcal{D}$  to produce the restored video  $\hat{x}_h$ .

#### 3.2. Joint Latent–Pixel Face-Focused Training

We observe that backgrounds in facial datasets are typically blurred with limited learnable information, while facial regions contain the most visually critical features for enhancement tasks. Therefore, we propose a Joint Latent–Pixel Face-Focused Training strategy that explicitly directs the model’s optimization toward key facial areas in both latent and pixel spaces.

To enable effective face-focused supervision in latent space, we construct facial masks that are spatially downsampled and temporally aggregated to match the resolution and frame rate of the VAE encoder’s latent representation. Specifically, given an input video  $x_l \in \mathbb{R}^{(1+T) \times H \times W \times 3}$ , we obtain its latent encoding  $z_l = \mathcal{E}(x_l) \in \mathbb{R}^{C \times T' \times H' \times W'}$ , where  $C = 16$ ,  $H' = H/8$ ,  $W' = W/8$ , and  $T' = 1+T/4$ . Our goal is to produce facial masks at the latent resolution that align spatially and temporally with  $z_l$ . Instead of encoding masks directly through the VAE, which would be computationally expensive, we adopt an efficient geometric alignment strategy. As illustrated in Fig. 2 (middle), per-frame binary facial masks  $M_p \in \{0, 1\}^{(1+T) \times H \times W}$  are extracted from the high-quality ground truth video  $x_h$  using a face parsing model [49]. We then spatially downsample these masks by a factor of 8 using nearest-neighbor interpolation to obtain:

$$\widetilde{M} = \mathcal{D}_s(M_p) \in [0, 1]^{(1+T) \times H' \times W'}. \quad (4)$$

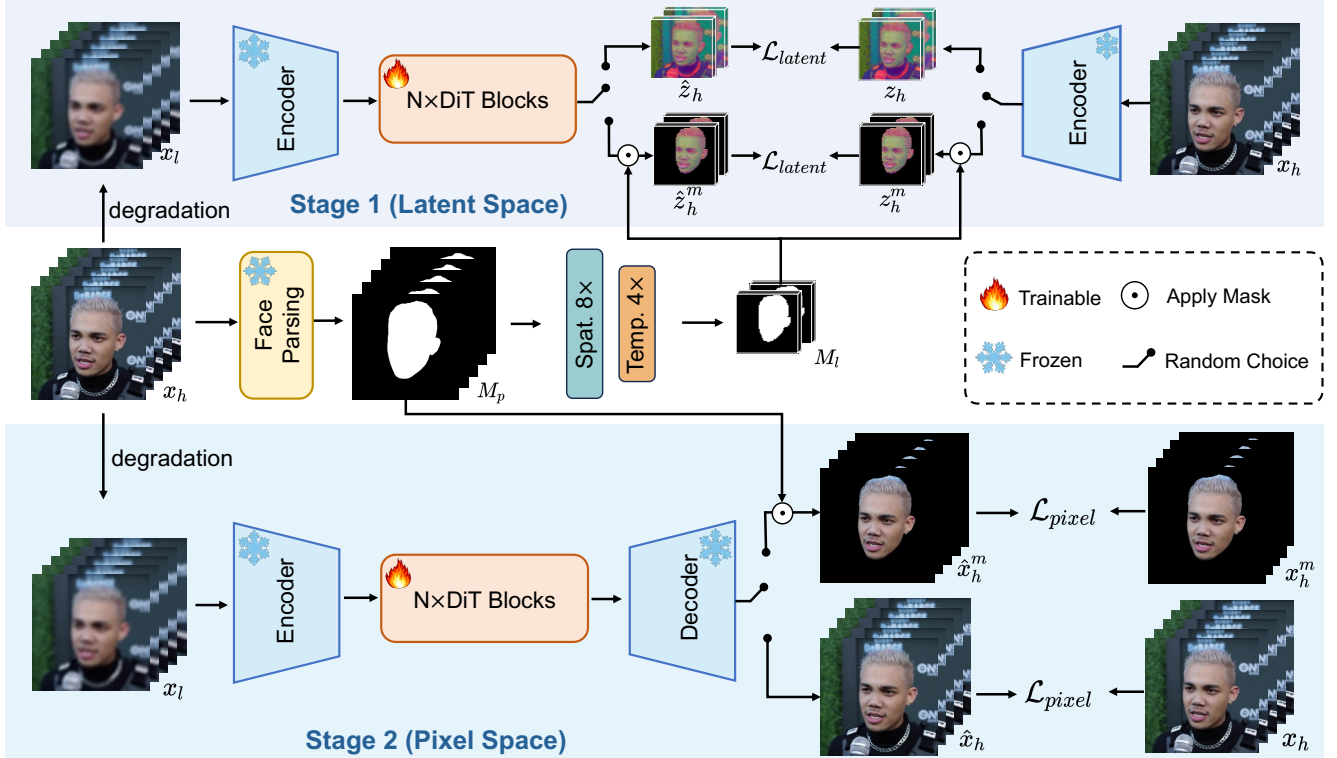


Figure 2. Overview of our proposed VividFace training framework. VividFace is a one-step diffusion method built upon the powerful WANX video model. It adopts a two-stage design that integrates latent and pixel-space optimization, leveraging spatiotemporal priors and stochastic training to simultaneously enhance facial details and overall video quality.

Next, temporal alignment is performed to match the encoder’s temporal compression. For latent temporal indices  $i = 0, \dots, T' - 1$ , we set  $\widehat{M}^{(0)} = \widetilde{M}^{(0)}$  for the first frame, while subsequent frames aggregate every four consecutive frames through element-wise maximum operation:

$$\widehat{M}^{(i)} = \max_{j=1}^4 \widetilde{M}^{(4(i-1)+j)}, \quad i = 1, \dots, T' - 1. \quad (5)$$

This process yields a spatiotemporally aligned facial mask  $\widehat{M} \in [0, 1]^{T' \times H' \times W'}$ , which is then replicated along the channel dimension to produce  $M_l \in [0, 1]^{C \times T' \times H' \times W'}$  that matches the shape of the latent representation  $z_l$ .

With the facial masks properly constructed, we incorporate them into our training framework using a stochastic strategy that randomly switches between face-focused and global reconstruction objectives. This balanced stochastic approach proves effective, outperforming both pure face-focused and pure global training alternatives (see ablation in Table 4). Formally, for a given representation space with ground-truth  $y$ , prediction  $\hat{y}$ , and mask  $M$ , the loss function is defined as:

$$\mathcal{L}(y, \hat{y}, M) = b \cdot \|M \odot (\hat{y} - y)\|_2^2 + (1 - b) \cdot \|\hat{y} - y\|_2^2, \quad (6)$$

where  $\odot$  denotes element-wise multiplication, and  $b \sim \text{Bernoulli}(p)$  is a binary random variable that stochasti-

cally selects between face-focused supervision ( $b = 1$ ) and global reconstruction ( $b = 0$ ) with probability  $p$ .

To accelerate convergence and enhance optimization stability, we design a progressive two-stage training strategy that leverages the complementary strengths of latent and pixel spaces. In the first stage, the model learns to fit the one-step flow trajectory by optimizing the latent space loss:

$$\mathcal{L}_{latent} = \mathcal{L}(z_h, \hat{z}_h, M_l), \quad (7)$$

where  $z_h$  and  $\hat{z}_h$  represent the latent representations of the target and predicted, respectively, and  $M_l$  is the facial mask in latent space. By operating directly in the compressed latent manifold, the model efficiently captures essential facial geometry and motion patterns before proceeding to pixel-level refinement. In the second stage, fine-tuning is performed in pixel space using a combination of MSE and perceptual losses:

$$\mathcal{L}_{pixel} = \mathcal{L}(x_h, \hat{x}_h, M_p) + \lambda \mathcal{L}_{DISTS}(x_h, \hat{x}_h), \quad (8)$$

where  $x_h$  and  $\hat{x}_h$  are the ground-truth and predicted RGB images,  $M_p$  is the facial mask in pixel space, and  $\mathcal{L}_{DISTS}$  [7] is a perceptual loss that enhances fine-grained detail generation. This hierarchical optimization leverages latent-space

learning efficiency to establish robust structural foundations, followed by targeted pixel-space refinement that enhances perceptual fidelity, resulting in superior restoration quality (see effectiveness in Section 4.2).

### 3.3. MLLM-Driven High-Quality Video Filtering

Existing face-centric datasets such as VFHQ suffer from two critical limitations: (1) facial regions occupy only a small portion of each frame, causing models to overfit to background reconstruction rather than learning fine-grained facial texture representations; (2) many video exhibit severe degradations, including motion blur, poor illumination, and occlusions. The quality of training data fundamentally determines the upper bound of model performance. Training on such degraded samples leads to outputs with unrealistic textures, as models cannot reproduce what they have never seen in high quality.

Based on these observations, we propose a novel MLLM-driven high-quality video filtering pipeline. This pipeline produces a curated, face-centric dataset called **MLLM-Face90**, as illustrated in Fig. 3.

**Face Region Extraction.** We employ a robust face parsing model [49] to segment each frame and extract tight bounding boxes around facial regions. To maintain spatial consistency across the video sequence, we aggregate all per-frame bounding boxes into a unified crop window that encompasses the face throughout all frames. This global window is then adjusted to a square shape to prevent facial distortion during subsequent resizing to square training dimensions. Finally, each frame is cropped according to this unified bounding box and resized to the target training dimensions. This procedure effectively eliminates background interference while preserving facial geometry integrity for subsequent quality assessment and model training.

**MLLM-Driven Quality Assessment and Filtering.** To ensure high-quality training data, we design an automated quality assessment pipeline using Qwen2.5-VL [1] with a meticulously crafted evaluation protocol specifically tailored for face restoration. Our protocol evaluates five critical dimensions: (1) facial detail clarity, (2) video stability and regional motion blur, (3) lighting quality, (4) compression artifacts and noise, and (5) facial occlusion. Each dimension is scored following strict rubrics, with bonus or penalty adjustments for outstanding quality or evident deficiencies. The protocol explicitly prioritizes critical facial regions (eyes, mouth, teeth, nose), penalizing motion blur or degradation in these areas while requiring natural lighting and artifact-free quality (see complete prompt in Supplementary Material Section B). Only videos achieving an overall quality score above 90 out of 100 are retained, forming our curated benchmark dataset, **MLLM-Face90**. Fine-tuning on MLLM-Face90 leads to substantial performance improvements, as shown in Table 6.

## 4. Experiments

### 4.1. Implementation details

**Training Details.** We adopt a coarse-to-fine strategy: first, 3,000 clips randomly sampled from VFHQ [43] are used for coarse training, followed by fine-tuning on MLLM-Face90, a curated set of 1,957 high-quality clips. To simulate real-world degradations, we follow [11] to synthesize low-quality data:  $y = [(x \circledast k_\sigma) \downarrow_r + n_\delta]_{\text{FFMPEG}_{\text{crf}}}$ , where  $x$ ,  $y$  are high- and low-quality videos.  $\circledast$  represents convolution,  $k_\sigma$  and  $n_\delta$  are the Gaussian blur kernel and noise, and  $\downarrow_r$  indicates  $r \times$  downsampling. During synthesis,  $\sigma$ ,  $r$ ,  $\delta$ , and  $\text{crf}$  are randomly sampled from  $[0.1, 10]$ ,  $[1, 4]$ ,  $[0, 10]$ , and  $[18, 25]$ , respectively. The hyperparameters  $\lambda$  and  $p$  are empirically set to 0.1 and 0.5, respectively. The frame resolutions for latent and pixel training stages are  $81 \times 512 \times 512$  and  $13 \times 512 \times 512$ . All experiments are conducted on eight NVIDIA A100 GPUs, with a batch size of 32 and a learning rate of  $1 \times 10^{-4}$  for a total of 32,000 iterations.

**Evaluation.** To comprehensively validate VividFace, we test on both synthetic and real-world benchmarks. For synthetic evaluation, following previous work, we use the official VFHQ-test dataset [43] with the aforementioned degradation model, containing 50 high-quality video clips. For real-world evaluation, we follow prior protocols using RFV-LQ [39]. RFV-LQ contains 329 low-quality face videos meticulously curated from diverse real-world sources, including old talk shows, TV series, and movies, providing a robust testbed for evaluating the method’s robustness across various real-world conditions.

**Metrics.** To facilitate a comprehensive and rigorous evaluation, we employ a diverse set of video quality assessment metrics spanning multiple dimensions of model performance. Specifically, we assess results from three key perspectives: Quality and Fidelity, Pose Consistency, and Temporal Consistency. For Quality and Fidelity, we use six representative metrics: PSNR, SSIM [38], and LPIPS [51] (reference-based), as well as NIQE [18], MUSIQ [13], and CLIP-IQA [30] (no-reference). To measure Pose Consistency, we adopt IDS, AKD, and FaceCons [10], as well as TLME [45]. We multiply AKD and TLME by 1000, denoted as AKD\* and TLME\*, respectively. For Temporal Consistency, we employ FasterVQA [41] and FVD [28].

**Compared Methods.** We evaluate our approach against three distinct categories of classic and representative compared methods. First, we select widely-used Video Super-Resolution (VSR) models, including BasicVSR++ [2], RealBasicVSR [3], MGLD-VSR [48], STAR [44], SeedVR-3B [32], and SeedVR2-3B [31]. Second, we include established Face Image-based Restoration (FIR) models, such as CodeFormer [53] and DiffFace [50], which restore facial details independently for each frame. Third, we compare with state-of-the-art Face Video Restoration (FVR) models

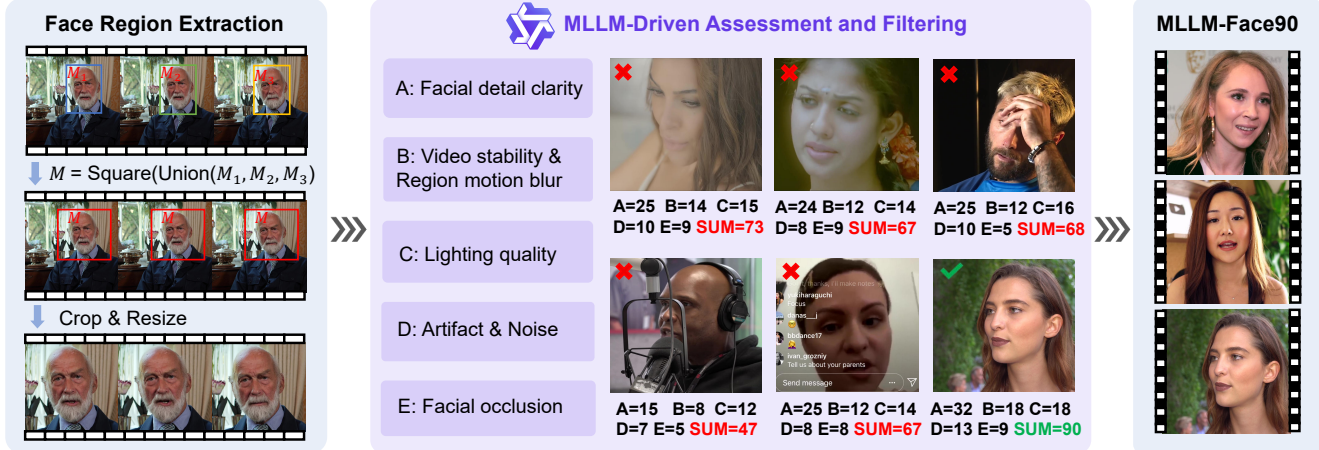


Figure 3. Pipeline of the proposed MLLM-driven high-quality face video filtering. First, face regions are extracted and cropped to facilitate the model’s focus on facial features. Next, a meticulously designed set of visual quality assessment prompts is utilized to evaluate each video from multiple quality perspectives using the powerful Qwen2.5-VL.

Table 1. Quantitative comparison on the **VFHQ-test** dataset. The best and second-best methods are highlighted in **red** and **blue** respectively. VividFace achieves superior performance across all metrics.

Method	Quality and Fidelity			Pose Consistency			Temporal Consistency	
	PSNR↑	SSIM↑	LPIPS↓	IDS↑	AKD*↓	FaceCons↑	FasterVQA↑	FVD↓
BasicVSR++[2]	25.64	0.7860	0.3902	0.7796	9.2778	0.7475	0.2108	1073.70
RealBasicVSR[3]	26.82	0.7793	0.2656	0.8046	6.3262	0.7442	0.8086	308.90
MGLD-VSR[48]	27.37	0.8111	0.2151	0.8350	4.6829	0.7297	0.7977	285.30
STAR[44]	24.66	0.7729	0.3393	0.8077	6.6215	0.7605	0.6643	464.51
SeedVR-3B[32]	27.04	0.7860	0.2271	0.8523	4.4892	0.7905	0.8025	126.14
SeedVR2-3B[31]	27.75	0.8420	<b>0.1538</b>	<b>0.8887</b>	3.9975	0.8013	0.8194	116.56
PGTFormer[46]	<b>28.78</b>	<b>0.8460</b>	0.1837	0.8612	4.3572	0.7298	<b>0.8484</b>	197.02
BFVR-STC[37]	24.37	0.7858	0.3383	0.7793	8.2443	0.7179	0.4594	700.20
KEEP[11]	27.50	0.8152	0.2376	0.7950	4.5966	0.7529	0.7986	388.60
SVFR[40]	28.09	0.8304	0.1578	0.8641	4.0932	<b>0.8025</b>	0.8404	<b>103.32</b>
DicFace[4]	28.25	0.8313	0.2424	0.8854	<b>3.9682</b>	0.7634	0.7207	340.76
<b>VividFace (Ours)</b>	<b>30.03</b>	<b>0.8534</b>	<b>0.1112</b>	<b>0.9128</b>	<b>3.5319</b>	<b>0.8111</b>	<b>0.8855</b>	<b>79.14</b>

including PGTFormer [46], BFVR-STC [37], KEEP [11], SVFR [40], and DicFace [4]. For all experiments, we use the same degradation settings and official implementations. For methods restricted to processing aligned facial regions, including CodeFormer, DiffFace, KEEP, and DicFace, we adopt a unified approach following the KEEP pipeline. The background is first enhanced using ESRGAN [33], and then composited back into the original frames.

## 4.2. Comparison with State-of-the-Art

**Quantitative Results.** We present a comprehensive performance comparison on the VFHQ-test benchmark in Table 1 and the real-world RFV-LQ benchmark in Table 2. VividFace demonstrates outstanding results, consistently surpass-

ing both VSR and FVR methods across all evaluation metrics. Specifically, in Table 1, VividFace significantly outperforms previous methods in PSNR, LPIPS, and FVD, achieving consistent superiority across multiple metrics. In Table 2, diverse no-reference video quality assessment metrics further confirm its robustness and superior visual quality in real-world scenarios. Additional comparisons with FIR methods are provided in the Supplementary Material (Table 7) show VividFace achieves notably higher temporal consistency, highlighting the effectiveness of our approach.

**Qualitative Results.** Comprehensive qualitative results on the VFHQ-test and real-world RFV-LQ datasets are presented in Figure 4 and Figure 5. Existing methods often produce blurred or over-smoothed outputs, struggling to re-

Table 2. Quantitative comparison on the **real-world** RFV-LQ dataset. The best and second-best methods are highlighted in **red** and **blue** respectively. Our method demonstrates superior performance in real-world scenarios.

Method	Quality and Fidelity			Pose Consistency		Temporal Consistency
	NIQE $\downarrow$	MUSIQ $\uparrow$	CLIP-IQA $\uparrow$	TLME* $\downarrow$	FaceCons $\uparrow$	FasterVQA $\uparrow$
BasicVSR++[2]	6.2983	30.8569	0.2005	7.3107	0.7207	0.2651
RealBasicVSR[3]	<b>5.0402</b>	63.1429	0.5407	6.5338	0.7392	0.7305
MGLD-VSR[48]	5.9269	62.7775	0.5593	6.2764	0.7359	0.7630
STAR	5.5227	<b>64.4846</b>	<b>0.5416</b>	6.4900	0.7222	0.7657
SeedVR-3B[32]	5.3900	52.8371	0.4759	6.6668	0.7430	0.6649
SeedVR2-3B[31]	6.6548	54.4296	0.4051	6.5437	<b>0.7593</b>	0.6059
PGTFormer[46]	6.7676	59.5214	0.4709	6.2961	0.7151	<b>0.7744</b>
BFVR-STC[37]	6.8477	45.5984	0.3372	6.7475	0.6928	0.5149
KEEP[11]	6.2016	60.9558	0.5054	<b>6.1623</b>	0.7392	0.7255
SVFR[40]	7.0772	54.2877	0.3907	6.1478	0.7527	0.6286
DicFace[4]	6.8448	53.9808	0.4525	6.2385	0.7413	0.6185
<b>VividFace (Ours)</b>	<b>5.1987</b>	<b>64.4911</b>	<b>0.5678</b>	<b>6.0064</b>	<b>0.7665</b>	<b>0.8227</b>

construct realistic structures in key regions such as the eyes, eyebrows, and mouth. In contrast, VividFace demonstrates superior capability in recovering more realistic and visually pleasing results: it faithfully restores fine-grained features while preserving surrounding facial structures, maintaining consistency with the ground-truth identity, and avoiding the over-smoothing artifacts observed in competing approaches. Additional qualitative results are provided in the **supplementary video files**.

**Running Time Comparisons.** Table 3 compares the inference speed and performance of several leading methods, all evaluated on identical hardware (single 80GB A100 GPU) using 81-frame 512 $\times$ 512 videos. Notably, VividFace completes inference in just **7.43 seconds**, being approximately **12 $\times$  faster** than SVFR and **2.7 $\times$  faster** than SeedVR2-3B, the closest one-step competitor. Importantly, VividFace achieves this speed without compromising perceptual quality or identity preservation, as evidenced by its superior LPIPS and IDS scores. These results highlight VividFace’s clear advantage in both efficiency and output fidelity.

Table 3. Running time comparison on 81-frame 512 $\times$ 512 videos across various methods. VividFace achieves the fastest inference speed while consistently delivering superior visual quality and better identity preservation compared to other approaches.

Method	Step	Time (s) $\downarrow$	LPIPS $\downarrow$	IDS $\uparrow$
MGLD-VSR[48]	50	98.73	0.215	0.835
STAR[44]	15	456.83	0.339	0.808
SeedVR-3B[32]	50	151.43	0.227	0.852
SeedVR2-3B[31]	1	19.98	0.153	0.888
SVFR[40]	30	94.60	0.157	0.864
<b>VividFace (Ours)</b>	<b>1</b>	<b>7.43</b>	<b>0.113</b>	<b>0.912</b>

### 4.3. Ablation Studies

**Effect of Face-Focused Training Probability  $p$ .** We investigate the impact of face-focused training probability  $p$  in Eq. 6, which controls the balance between face-focused and global reconstruction objectives. As shown in Table 4, we evaluate three different values: 0 (pure global training), 0.5 (balanced stochastic training), and 1 (pure face-focused training). The results demonstrate that  $p = 0.5$  achieves optimal performance. Pure global training leads to suboptimal facial detail recovery, while pure face-focused training compromises overall video quality due to insufficient global context learning. The balanced approach effectively combines both objectives.

Table 4. Effect of face-focused training probability  $p$ . The balanced probability  $p = 0.5$  achieves best performance through joint face-focused and global reconstruction.

$p$	LPIPS $\downarrow$	IDS $\uparrow$
0	0.1229	0.9073
<b>0.5</b>	<b>0.1112</b>	<b>0.9128</b>
1	0.1309	0.9025

### Effectiveness of Joint Latent-Pixel Training Strategy

We validate our Joint Latent-Pixel Face-Focused Training strategy by progressively adding training components. Table 5 presents three configurations: baseline without face-focused training, latent space only, and joint training in both spaces. Adding latent space training alone slightly degrades performance, suggesting that latent-only optimization is insufficient for fine-grained facial detail recovery. However, the complete joint training strategy significantly improves both metrics, demonstrating that multi-space optimization is crucial for optimal facial enhancement quality.



Figure 4. Visual comparison with existing methods on VFHQ-test. VividFace exhibits more realistic and visually pleasing facial details, and produces results that are closer to the ground truth.



Figure 5. Qualitative comparison on real-world RFV-LQ dataset. The results highlight VividFace’s strong capability to address complex real-world degradations.

Table 5. Ablation study on Joint Latent-Pixel Face-Focused Training. The joint training strategy clearly outperforms individual components, validating the necessity of multi-space optimization.

Latent	Pixel	LPIPS $\downarrow$	IDS $\uparrow$
$\times$	$\times$	0.1229	0.9073
$\checkmark$	$\times$	0.1261	0.9050
$\checkmark$	$\checkmark$	<b>0.1112</b>	<b>0.9128</b>

Table 6. Ablation study on the MLLM-Face90 dataset. Incorporating our high-quality curated dataset improves performance.

Dataset	LPIPS $\downarrow$	IDS $\uparrow$
VFHQ-3K	0.1285	0.9046
<b>+MLLM-Face90</b>	<b>0.1112</b>	<b>0.9128</b>

tion pipeline in providing high-quality face-centric training data for learning authentic facial textures.

## 5. Conclusion

In this work, we present VividFace, an efficient one-step diffusion framework that advances video face enhancement through three key innovations. First, by reformulating multi-step diffusion into single-step flow matching built upon the text-to-video model WANX, we achieve substan-

**Impact of MLLM-Face90 High-Quality Dataset.** We evaluate the contribution of our MLLM-Face90 dataset by comparing models trained on different data configurations. Table 6 compares using only VFHQ-3K versus incorporating our curated dataset. The incorporation of MLLM-Face90 leads to clear improvements across both metrics, validating the effectiveness of our MLLM-driven data cura-

tial efficiency gains without compromising visual fidelity. Second, our Joint Latent-Pixel Face-Focused Training strategy leverages spatiotemporally aligned facial masks to enable targeted optimization of critical facial regions across both representation spaces. Third, our MLLM-driven data curation pipeline facilitates automated construction of high-quality face video datasets, enhancing model generalization and robustness. Comprehensive evaluations validate the effectiveness of each component, with VividFace consistently outperforming existing methods across multiple benchmarks. We hope our released resources encourage further research on efficient generative video restoration.

## References

- [1] Shuai Bai, Keqin Chen, Xuejing Liu, Jialin Wang, Wenbin Ge, Sibo Song, Kai Dang, Peng Wang, Shijie Wang, Jun Tang, Humen Zhong, Yuanzhi Zhu, Mingkun Yang, Zhao-hai Li, Jianqiang Wan, Pengfei Wang, Wei Ding, Zheren Fu, Yiheng Xu, Jiabo Ye, Xi Zhang, Tianbao Xie, Zesen Cheng, Hang Zhang, Zhibo Yang, Haiyang Xu, and Junyang Lin. Qwen2.5-vl technical report. *arXiv preprint arXiv:2502.13923*, 2025. 5
- [2] Kelvin CK Chan, Shangchen Zhou, Xiangyu Xu, and Chen Change Loy. Basicvsr++: Improving video super-resolution with enhanced propagation and alignment. In *Proceedings of the IEEE/CVF conference on computer vision and pattern recognition*, pages 5972–5981, 2022. 2, 5, 6, 7
- [3] Kelvin CK Chan, Shangchen Zhou, Xiangyu Xu, and Chen Change Loy. Investigating tradeoffs in real-world video super-resolution. In *Proceedings of the IEEE/CVF conference on computer vision and pattern recognition*, pages 5962–5971, 2022. 2, 5, 6, 7
- [4] Yan Chen, Hanlin Shang, Ce Liu, Yuxuan Chen, Hui Li, Weihao Yuan, Hao Zhu, Zilong Dong, and Siyu Zhu. Dic-face: Dirichlet-constrained variational codebook learning for temporally coherent video face restoration. *arXiv preprint arXiv:2506.13355*, 2025. 2, 6, 7
- [5] Ziyan Chen, Jingwen He, Xinqi Lin, Yu Qiao, and Chao Dong. Towards real-world video face restoration: A new benchmark. In *Proceedings of the IEEE/CVF Conference on Computer Vision and Pattern Recognition*, pages 5929–5939, 2024. 2
- [6] Zheng Chen, Zichen Zou, Kewei Zhang, Xiongfei Su, Xin Yuan, Yong Guo, and Yulun Zhang. Dove: Efficient one-step diffusion model for real-world video super-resolution. *arXiv preprint arXiv:2505.16239*, 2025. 3
- [7] Keyan Ding, Kede Ma, Shiqi Wang, and Eero P. Simoncelli. Image quality assessment: Unifying structure and texture similarity. *CoRR*, abs/2004.07728, 2020. 4
- [8] Linwei Dong, Qingnan Fan, Yihong Guo, Zhonghao Wang, Qi Zhang, Jinwei Chen, Yawei Luo, and Changqing Zou. Tsd-sr: One-step diffusion with target score distillation for real-world image super-resolution. In *Proceedings of the Computer Vision and Pattern Recognition Conference*, pages 23174–23184, 2025. 3
- [9] Patrick Esser, Sumith Kulal, Andreas Blattmann, Rahim Entezari, Jonas Müller, Harry Saini, Yam Levi, Dominik Lorenz, Axel Sauer, Frederic Boesel, et al. Scaling rectified flow transformers for high-resolution image synthesis. In *Forty-first international conference on machine learning*, 2024. 2, 3
- [10] Ruicheng Feng, Chongyi Li, and Chen Change Loy. Kalman-inspired feature propagation for video face super-resolution. In *Computer Vision - ECCV 2024 - 18th European Conference, Milan, Italy, September 29–October 4, 2024, Proceedings, Part XXVI*, pages 202–218. Springer, 2024. 5
- [11] Ruicheng Feng, Chongyi Li, and Chen Change Loy. Kalman-inspired feature propagation for video face super-resolution. In *European Conference on Computer Vision*, pages 202–218. Springer, 2024. 2, 5, 6, 7
- [12] Jonathan Ho, Ajay Jain, and Pieter Abbeel. Denoising diffusion probabilistic models. *Advances in neural information processing systems*, 33:6840–6851, 2020. 3
- [13] Junjie Ke, Qifei Wang, Yilin Wang, Peyman Milanfar, and Feng Yang. Musiq: Multi-scale image quality transformer. In *Proceedings of the IEEE/CVF international conference on computer vision*, pages 5148–5157, 2021. 5
- [14] Jianze Li, Jiezhang Cao, Zichen Zou, Xiongfei Su, Xin Yuan, Yulun Zhang, Yong Guo, and Xiaokang Yang. Distillation-free one-step diffusion for real-world image super-resolution. *arXiv preprint arXiv:2410.04224*, 2024. 3
- [15] Yawei Li, Yulun Zhang, Radu Timofte, Luc Van Gool, Lei Yu, Youwei Li, Xinpeng Li, Ting Jiang, Qi Wu, Mingyan Han, et al. Ntire 2023 challenge on efficient super-resolution: Methods and results. In *Proceedings of the IEEE/CVF Conference on Computer Vision and Pattern Recognition*, pages 1922–1960, 2023. 2
- [16] Jingyun Liang, Jiezhang Cao, Yuchen Fan, Kai Zhang, Rakesh Ranjan, Yawei Li, Radu Timofte, and Luc Van Gool. VRT: A video restoration transformer. *CoRR*, abs/2201.12288, 2022. 2
- [17] Yong Liu, Jinshan Pan, Yinchuan Li, Qingji Dong, Chao Zhu, Yu Guo, and Fei Wang. Ultravsr: Achieving ultra-realistic video super-resolution with efficient one-step diffusion space. *arXiv preprint arXiv:2505.19958*, 2025. 3
- [18] Anish Mittal, Rajiv Soundararajan, and Alan C Bovik. Making a “completely blind” image quality analyzer. *IEEE Signal processing letters*, 20(3):209–212, 2012. 5
- [19] Arsha Nagrani, Joon Son Chung, Weidi Xie, and Andrew Zisserman. Voxceleb: Large-scale speaker verification in the wild. *Computer Speech & Language*, 60:101027, 2020. 2
- [20] Long Peng, Aiwen Jiang, Qiaosi Yi, and Mingwen Wang. Cumulative rain density sensing network for single image derain. *IEEE Signal Processing Letters*, 27:406–410, 2020. 2
- [21] Bin Ren, Yawei Li, Nancy Mehta, Radu Timofte, Hongyuan Yu, Cheng Wan, Yuxin Hong, Bingnan Han, Zhuoyuan Wu, Yajun Zou, et al. The ninth ntire 2024 efficient super-resolution challenge report. In *Proceedings of the IEEE/CVF Conference on Computer Vision and Pattern Recognition*, pages 6595–6631, 2024. 2

[22] Robin Rombach, Andreas Blattmann, Dominik Lorenz, Patrick Esser, and Björn Ommer. High-resolution image synthesis with latent diffusion models. In *Proceedings of the IEEE/CVF conference on computer vision and pattern recognition*, pages 10684–10695, 2022. 3

[23] Claudio Rota, Marco Buzzelli, Simone Bianco, and Raimondo Schettini. Video restoration based on deep learning: a comprehensive survey. *Artif. Intell. Rev.*, 56(6):5317–5364, 2023. 2

[24] Jiaming Song, Chenlin Meng, and Stefano Ermon. Denoising diffusion implicit models. *arXiv preprint arXiv:2010.02502*, 2020. 3

[25] Yang Song, Jascha Sohl-Dickstein, Diederik P Kingma, Abhishek Kumar, Stefano Ermon, and Ben Poole. Score-based generative modeling through stochastic differential equations. *arXiv preprint arXiv:2011.13456*, 2020. 3

[26] Yujing Sun, Lingchen Sun, Shuaizheng Liu, Rongyuan Wu, Zhengqiang Zhang, and Lei Zhang. One-step diffusion for detail-rich and temporally consistent video super-resolution. *arXiv preprint arXiv:2506.15591*, 2025. 3

[27] Jingfan Tan, Hyunhee Park, Ying Zhang, Tao Wang, Kaihao Zhang, Xiangyu Kong, Pengwen Dai, Zikun Liu, and Wenhan Luo. Blind face video restoration with temporal consistent generative prior and degradation-aware prompt. In *Proceedings of the 32nd ACM International Conference on Multimedia*, page 1417–1426, 2024. 2

[28] Thomas Unterthiner, Sjoerd van Steenkiste, Karol Kurach, Raphaël Marinier, Marcin Michalski, and Sylvain Gelly. FVD: A new metric for video generation. In *Deep Generative Models for Highly Structured Data, ICLR 2019 Workshop, New Orleans, Louisiana, United States, May 6, 2019*. OpenReview.net, 2019. 5

[29] Ang Wang, Baole Ai, Bin Wen, Chaojie Mao, Chen-Wei Xie, Di Chen, Feiwu Yu, Haiming Zhao, Jianxiao Yang, Jianyuan Zeng, Jiayu Wang, Jingfeng Zhang, Jingren Zhou, Jinkai Wang, Jixuan Chen, Kai Zhu, Kang Zhao, Keyu Yan, Lianghua Huang, Xiaofeng Meng, Ningyi Zhang, Pandeng Li, Pingyu Wu, Ruihang Chu, Ruili Feng, Shiwei Zhang, Siyang Sun, Tao Fang, Tianxing Wang, Tianyi Gui, Tingyu Weng, Tong Shen, Wei Lin, Wei Wang, Wei Wang, Wemmeng Zhou, Wente Wang, Wenting Shen, Wenyuan Yu, Xianzhong Shi, Xiaoming Huang, Xin Xu, Yan Kou, Yangyu Lv, Yifei Li, Yijing Liu, Yiming Wang, Yingya Zhang, Yitong Huang, Yong Li, You Wu, Yu Liu, Yulin Pan, Yun Zheng, Yuntao Hong, Yupeng Shi, Yutong Feng, Zeyinzi Jiang, Zhen Han, Zhi-Fan Wu, and Ziyu Liu. Wan: Open and advanced large-scale video generative models. *CoRR*, abs/2503.20314, 2025. 2, 3

[30] Jianyi Wang, Kelvin CK Chan, and Chen Change Loy. Exploring clip for assessing the look and feel of images. In *Proceedings of the AAAI conference on artificial intelligence*, pages 2555–2563, 2023. 5

[31] Jianyi Wang, Shanchuan Lin, Zhijie Lin, Yuxi Ren, Meng Wei, Zongsheng Yue, Shangchen Zhou, Hao Chen, Yang Zhao, Ceyuan Yang, Xuefeng Xiao, Chen Change Loy, and Lu Jiang. Seedvr2: One-step video restoration via diffusion adversarial post-training. *CoRR*, abs/2506.05301, 2025. 3, 5, 6, 7

[32] Jianyi Wang, Zhijie Lin, Meng Wei, Yang Zhao, Ceyuan Yang, Chen Change Loy, and Lu Jiang. Seedvr: Seeding infinity in diffusion transformer towards generic video restoration. In *CVPR*, 2025. 2, 5, 6, 7

[33] Xintao Wang, Liangbin Xie, Chao Dong, and Ying Shan. Real-esrgan: Training real-world blind super-resolution with pure synthetic data. In *Proceedings of the IEEE/CVF international conference on computer vision*, pages 1905–1914, 2021. 6

[34] Yang Wang, Long Peng, Liang Li, Yang Cao, and Zheng-Jun Zha. Decoupling-and-aggregating for image exposure correction. In *Proceedings of the IEEE/CVF conference on computer vision and pattern recognition*, pages 18115–18124, 2023. 2

[35] Yufei Wang, Wenhan Yang, Xinyuan Chen, Yaohui Wang, Lanqing Guo, Lap-Pui Chau, Ziwei Liu, Yu Qiao, Alex C Kot, and Bihan Wen. Sinsr: diffusion-based image super-resolution in a single step. In *Proceedings of the IEEE/CVF conference on computer vision and pattern recognition*, pages 25796–25805, 2024. 3

[36] Yingqian Wang, Zhengyu Liang, Fengyuan Zhang, Lvli Tian, Longguang Wang, Juncheng Li, Jungang Yang, Radu Timofte, Yulan Guo, Kai Jin, et al. Ntire 2025 challenge on light field image super-resolution: Methods and results. In *Proceedings of the Computer Vision and Pattern Recognition Conference*, pages 1227–1246, 2025. 2

[37] Yutong Wang, Jiajie Teng, Jiajiong Cao, Yuming Li, Chenguang Ma, Hongteng Xu, and Dixin Luo. Efficient video face enhancement with enhanced spatial-temporal consistency. In *Proceedings of the Computer Vision and Pattern Recognition Conference*, pages 2183–2193, 2025. 2, 6, 7

[38] Zhou Wang, Alan C Bovik, Hamid R Sheikh, and Eero P Simoncelli. Image quality assessment: from error visibility to structural similarity. *IEEE transactions on image processing*, 13(4):600–612, 2004. 5

[39] Zhouxia Wang, Jiawei Zhang, Xintao Wang, Tianshui Chen, Ying Shan, Wenping Wang, and Ping Luo. Analysis and benchmarking of extending blind face image restoration to videos. *IEEE Transactions on Image Processing*, 2024. 5

[40] Zhiyao Wang, Xu Chen, Chengming Xu, Junwei Zhu, Xiaobin Hu, Jiangning Zhang, Chengjie Wang, Yuqi Liu, Yiyi Zhou, and Rongrong Ji. Svfr: A unified framework for generalized video face restoration. In *Proceedings of the Computer Vision and Pattern Recognition Conference*, pages 7406–7415, 2025. 2, 6, 7

[41] Haoning Wu, Chaofeng Chen, Liang Liao, Jingwen Hou, Wenxiu Sun, Qiong Yan, Jinwei Gu, and Weisi Lin. Neighbourhood representative sampling for efficient end-to-end video quality assessment. *IEEE Transactions on Pattern Analysis and Machine Intelligence*, 45(12):15185–15202, 2023. 5

[42] Rongyuan Wu, Lingchen Sun, Zhiyuan Ma, and Lei Zhang. One-step effective diffusion network for real-world image super-resolution. *Advances in Neural Information Processing Systems*, 37:92529–92553, 2024. 3

[43] Liangbin Xie, Xintao Wang, Honglun Zhang, Chao Dong, and Ying Shan. Vfhq: A high-quality dataset and benchmark for video face super-resolution. In *Proceedings of*

*the IEEE/CVF Conference on Computer Vision and Pattern Recognition*, pages 657–666, 2022. [2](#), [5](#)

- [44] Rui Xie, Yinhong Liu, Penghao Zhou, Chen Zhao, Jun Zhou, Kai Zhang, Zhenyu Zhang, Jian Yang, Zhenheng Yang, and Ying Tai. Star: Spatial-temporal augmentation with text-to-video models for real-world video super-resolution, 2025. [2](#), [5](#), [6](#), [7](#)
- [45] Kepeng Xu, Li Xu, Gang He, Wenxin Yu, and Yunsong Li. Beyond alignment: Blind video face restoration via parsing-guided temporal-coherent transformer. In *Proceedings of the Thirty-Third International Joint Conference on Artificial Intelligence, IJCAI 2024, Jeju, South Korea, August 3-9, 2024*, pages 1489–1497. ijcai.org, 2024. [5](#)
- [46] Kepeng Xu, Li Xu, Gang He, Wenxin Yu, and Yunsong Li. Beyond alignment: Blind video face restoration via parsing-guided temporal-coherent transformer. *arXiv preprint arXiv:2404.13640*, 2024. [2](#), [6](#), [7](#)
- [47] Yipiao Xu, Zhenbo Song, and Jianfeng Lu. Universal video face restoration method based on vision-language model. In *The 16th Asian Conference on Machine Learning (Conference Track)*, 2024. [2](#)
- [48] Xi Yang, Chenhang He, Jianqi Ma, and Lei Zhang. Motion-guided latent diffusion for temporally consistent real-world video super-resolution. In *European conference on computer vision*, pages 224–242. Springer, 2024. [2](#), [5](#), [6](#), [7](#)
- [49] Changqian Yu, Jingbo Wang, Chao Peng, Changxin Gao, Gang Yu, and Nong Sang. Bisenet: Bilateral segmentation network for real-time semantic segmentation. In *Proceedings of the European conference on computer vision (ECCV)*, pages 325–341, 2018. [3](#), [5](#)
- [50] Zongsheng Yue and Chen Change Loy. Difface: Blind face restoration with diffused error contraction. *IEEE Transactions on Pattern Analysis and Machine Intelligence*, 2024. [5](#), [2](#)
- [51] Richard Zhang, Phillip Isola, Alexei A Efros, Eli Shechtman, and Oliver Wang. The unreasonable effectiveness of deep features as a perceptual metric. In *Proceedings of the IEEE conference on computer vision and pattern recognition*, pages 586–595, 2018. [5](#)
- [52] Xi Zhang and Xiaolin Wu. Multi-modality deep restoration of extremely compressed face videos. *CoRR*, abs/2107.05548, 2021. [2](#)
- [53] Shangchen Zhou, Kelvin Chan, Chongyi Li, and Chen Change Loy. Towards robust blind face restoration with codebook lookup transformer. *Advances in Neural Information Processing Systems*, 35:30599–30611, 2022. [5](#), [2](#)
- [54] Hao Zhu, Wayne Wu, Wentao Zhu, Liming Jiang, Siwei Tang, Li Zhang, Ziwei Liu, and Chen Change Loy. CelebV-HQ: A large-scale video facial attributes dataset. In *ECCV*, 2022. [2](#)
- [55] Zihao Zou, Jiaming Liu, Shirin Shoushtari, Yubo Wang, and Ulugbek S. Kamilov. FLAIR: A conditional diffusion framework with applications to face video restoration. In *IEEE/CVF Winter Conference on Applications of Computer Vision, WACV 2025, Tucson, AZ, USA, February 26 - March 6, 2025*, pages 5228–5238. IEEE, 2025. [2](#)

# VividFace: High-Quality and Efficient One-Step Diffusion For Video Face Enhancement

## Supplementary Material

### A. More visual and performance comparison

**More qualitative comparisons with face restoration methods.** Figure 6 presents additional qualitative comparisons on the VFHQ-test dataset. As illustrated, our VividFace faithfully recovers skin details such as wrinkles and texture around the eye region. These results further validate the capability of VividFace to achieve photorealistic facial enhancement.

**More performance comparisons with face restoration methods.** As shown in Table 7, FIR methods exhibit substantially inferior performance compared to our video-aware approach across all evaluation dimensions. Notably, while FIR methods achieve reasonable per-frame quality metrics, they suffer from severe degradation in pose consistency and catastrophic failure in temporal coherence. DiffFace, despite being a recent diffusion-based method, shows particularly poor identity preservation and facial geometry consistency, suggesting that frame-independent stochastic generation fundamentally lacks the temporal modeling required for video restoration. These results demonstrate the critical importance of video-aware processing and validate the exceptional capability of our approach in maintaining spatio-temporal consistency for face video restoration.

**Visualization of temporal consistency comparison.** Temporal consistency is a crucial aspect of video enhancement. Therefore, we further compare the temporal consistency performance of existing methods, as shown in Figure 7. Specifically, we select the region marked by the red line and display its continuous representations across different frames. It can be observed that VividFace demonstrates superior temporal consistency with significantly reduced jitter compared to other approaches, and its results are much closer to the ground truth.

### B. MLLM Prompt for Video Quality Assessment

In this section, we present the detailed prompt used for multi-dimensional video quality assessment. The prompt evaluates videos across five key dimensions: **facial detail clarity, video stability and motion blur, lighting quality, artifact and noise level, and facial occlusion**. It employs a comprehensive 100-point scoring system with bonus and penalty mechanisms to ensure rigorous selection of premium training data.

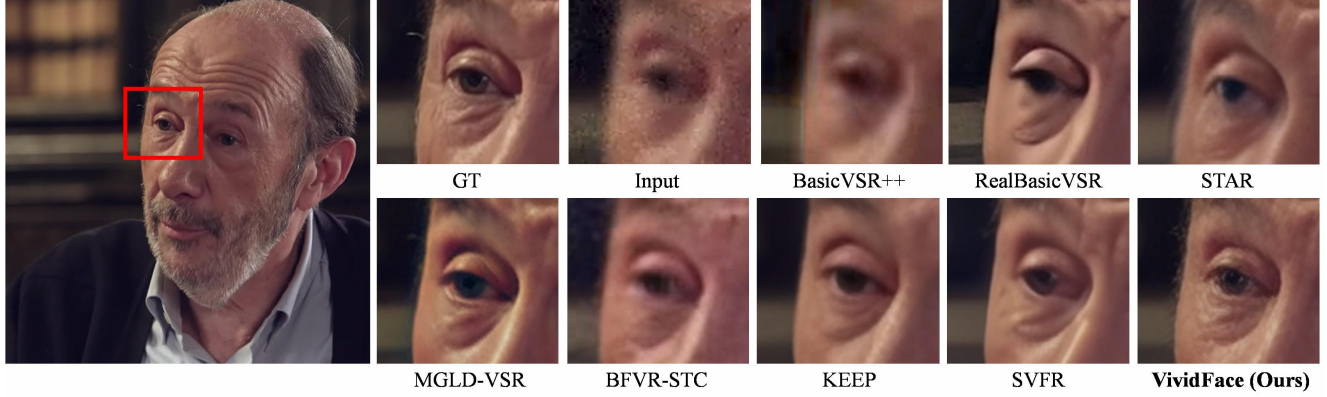


Figure 6. More qualitative comparison on VFHQ-test dataset. VividFace effectively recovers subtle skin details and enhances perceptual quality.

Table 7. Comparisons of face image restoration (FIR) methods on the VFHQ-test dataset.

Method	Quality and Fidelity			Pose Consistency			Temporal Consistency	
	PSNR↑	SSIM↑	LPIPS↓	IDS↑	AKD*↓	FaceCons↑	FasterVQA↑	FVD↓
FIR	CodeFormer [53]	27.27	0.8023	0.2391	0.7719	5.5370	0.7156	0.8625
	DifFace [50]	26.73	0.7919	0.2538	0.5998	7.6810	0.4544	0.8278
<b>VividFace (Ours)</b>	<b>30.03</b>	<b>0.8534</b>	<b>0.1112</b>	<b>0.9128</b>	<b>3.5319</b>	<b>0.8111</b>	<b>0.8855</b>	<b>79.14</b>

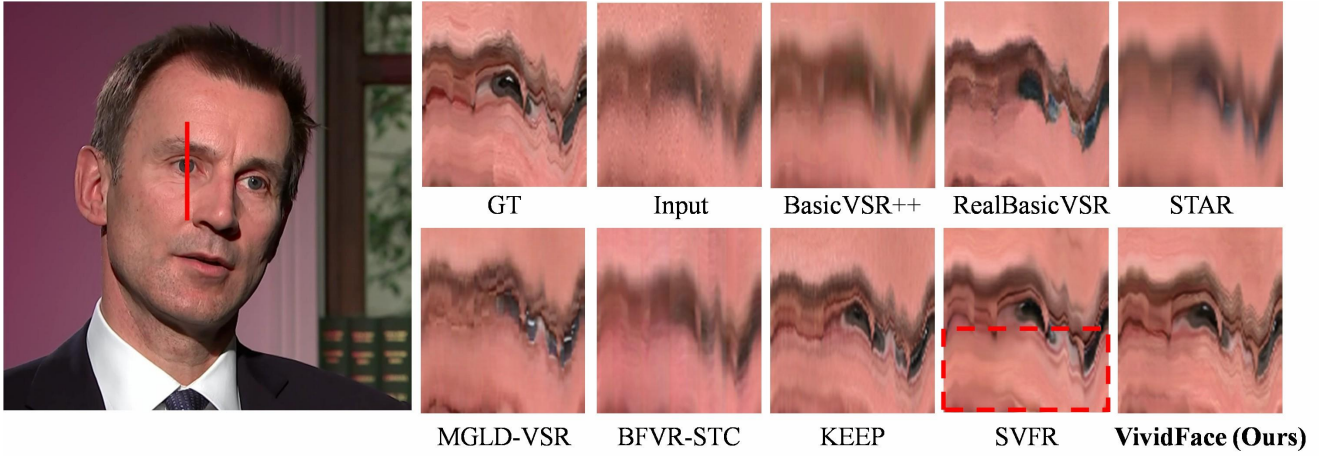


Figure 7. Visualization of temporal consistency comparison. VividFace achieves temporal results that are closer to the ground truth, verifying its stronger temporal consistency.

#### Premium Face Video Quality Evaluation Prompt

You are an expert face video quality inspector specializing in premium face restoration training data. Evaluate this video with **STRICT** criteria to identify only the highest quality samples suitable for premium model training.

##### **Evaluation Criteria (Total: 100 points) - STRICT GRADING:**

###### **1. Facial Detail Clarity (35 points)**

- 0-12: Severely degraded, facial features barely distinguishable
- 13-21: Moderate quality, basic features visible but lacking fine details
- 22-28: Good quality with visible skin texture and facial features, BUT penalize if key regions (eyes, mouth, teeth) show motion blur
- 29-32: Excellent clarity with clear pores, fine lines, and detailed texture across ALL facial regions
- 33-35: Perfect clarity with crisp micro-details (individual eyelashes, teeth edges, lip texture clearly visible)

###### **2. Video Stability & Regional Motion Blur (20 points)**

- 0-6: Severe motion blur or instability affecting entire face
- 7-11: Noticeable camera shake OR significant motion blur in key facial regions (eyes, mouth, teeth)
- 12-15: Minor overall stability issues, but critical facial features remain sharp
- 16-18: Very stable with minimal motion blur, all key facial regions clear
- 19-20: Perfect stability across all frames, no motion blur in any facial region

###### **3. Lighting Quality (20 points)**

- 0-6: Extreme lighting conditions that obscure facial features
- 7-11: Acceptable lighting with noticeable issues (uneven shadows, slight over/under exposure)
- 12-15: Good lighting with minor imperfections
- 16-18: Excellent natural lighting with proper facial modeling
- 19-20: Perfect studio-quality lighting with optimal facial structure revelation

###### **4. Artifact & Noise Level (15 points)**

- 0-4: Heavy compression artifacts, noise, or digital distortions
- 5-7: Noticeable artifacts that affect facial details
- 8-10: Minor artifacts present but don't significantly impact quality
- 11-13: Minimal artifacts, high video quality

- 14-15: No visible artifacts, pristine video quality

#### 5. Facial Occlusion (10 points)

- 0-2: Significant occlusion (>25% of face covered by objects, hands)
- 3-4: Moderate occlusion (10-25% covered)
- 5-6: Minor occlusion (5-10% covered), most facial features visible
- 7-8: Minimal occlusion (<5% covered), all key facial features clearly visible
- 9-10: No occlusion, complete facial visibility

#### Critical Facial Regions Check:

- Eyes: Must be sharp with visible iris details, eyelashes clearly defined
- Mouth/Lips: Lip texture and edges must be crisp, no blur during speech
- Teeth: Individual teeth edges must be clearly visible when shown
- Nose: Nostril details and nose bridge must be sharp

#### STRICT QUALITY THRESHOLDS:

- Premium Training Data: Score >= 85 (Top 10-15% of videos)
- High-Quality Training Data: Score >= 80 (Top 20-25% of videos)
- Standard Training Data: Score >= 75 (Top 40% of videos)
- Below Standard: Score < 75 (Consider discarding for premium training)

#### Additional Quality Factors (Bonus/Penalty):

- **Bonus (+2 points):** Exceptional skin texture detail visible throughout video
- **Bonus (+1 point):** Perfect color reproduction and white balance
- **Penalty (-3 points):** Motion blur detected in ANY key facial region (eyes, mouth, teeth) even if brief
- **Penalty (-2 points):** Any visible digital noise or grain
- **Penalty (-3 points):** Unnatural skin smoothing or beauty filter effects
- **Penalty (-2 points):** Inconsistent sharpness between frames (some frames sharp, others blurry)

#### EVALUATION PROCESS – FOLLOW THESE STEPS:

1. First, evaluate each criteria and assign a specific score:

- Clarity: \_\_\_/35
- Stability: \_\_\_/20
- Lighting: \_\_\_/20
- Artifacts: \_\_\_/15
- Occlusion: \_\_\_/10

2. Calculate the base score by adding the five scores above:

Base Score = Clarity + Stability + Lighting + Artifacts + Occlusion = \_\_\_

3. Apply bonus/penalty adjustments:

- List each bonus/penalty with the reason
- Calculate adjustment total: \_\_\_
- Final Score = Base Score + Adjustment = \_\_\_

4. Determine quality tier based on final score

#### MANDATORY OUTPUT FORMAT:

##### STEP 1 – Individual Scores:

Clarity: X/35 (reason for score)  
 Stability: X/20 (reason for score)  
 Lighting: X/20 (reason for score)  
 Artifacts: X/15 (reason for score)  
 Occlusion: X/10 (reason for score)

##### STEP 2 – Base Score Calculation:

Base Score = X + X + X + X + X = X/100

STEP 3 - Bonus/Penalty Adjustments:

[List each bonus/penalty with reason and points]

Total Adjustment: +/-X points

STEP 4 - Final Results:

Final Score = X (Base) + X (Adjustment) = X/100

Quality Tier: [Premium/High/Standard/Below Standard]

Critical Issues: [List any issues that prevent premium quality classification]

Motion Blur Check: [Specifically note if eyes/mouth/teeth show any motion blur]

**IMPORTANT GRADING NOTES:**

- Be exceptionally strict with scoring - err on the side of lower scores
- Only award top scores (90+) for truly exceptional, near-perfect quality
- Consider that this is for premium training data - standards are higher than typical use
- Focus on details that would be critical for face restoration model performance
- Penalize any imperfections that could negatively impact training effectiveness
- DOUBLE-CHECK your arithmetic at each step to ensure accuracy

Please provide a complete evaluation following the exact format above, including all calculation steps.